



## Assessment of the inflatable core assisted paper bottle moulding process

Saxena, Prateek; Bissacco, Giuliano

*Published in:*  
Procedia Manufacturing

*Link to article, DOI:*  
[10.1016/j.promfg.2019.04.038](https://doi.org/10.1016/j.promfg.2019.04.038)

*Publication date:*  
2019

*Document Version*  
Publisher's PDF, also known as Version of record

[Link back to DTU Orbit](#)

*Citation (APA):*  
Saxena, P., & Bissacco, G. (2019). Assessment of the inflatable core assisted paper bottle moulding process. *Procedia Manufacturing*, 33, 312-318. <https://doi.org/10.1016/j.promfg.2019.04.038>

---

### General rights

Copyright and moral rights for the publications made accessible in the public portal are retained by the authors and/or other copyright owners and it is a condition of accessing publications that users recognise and abide by the legal requirements associated with these rights.

- Users may download and print one copy of any publication from the public portal for the purpose of private study or research.
- You may not further distribute the material or use it for any profit-making activity or commercial gain
- You may freely distribute the URL identifying the publication in the public portal

If you believe that this document breaches copyright please contact us providing details, and we will remove access to the work immediately and investigate your claim.



16th Global Conference on Sustainable Manufacturing - Sustainable Manufacturing for Global Circular Economy

# Assessment of the inflatable core assisted paper bottle moulding process

Prateek Saxena\*, Giuliano Bissacco

*Department of Mechanical Engineering, Technical University of Denmark, Kgs. Lyngby 2800, Denmark*

---

## Abstract

Eco-friendly products have gained importance in recent years. The paper bottle is a sustainable packaging solution for carbonated beverages. The moulding process is a two-stage process. At first, pulp is poured in the forming mould and fibers are formed in the desired shape. Wet bottle is then transferred to the drying mould to remove bound water. The drying process makes use of an inflatable core, which not only prevents the shrinkage of fibers but also helps in attaining good fiber compaction. Preliminary investigations reported uneven fiber compaction in changing curvatures and sharp corners. A cause of uneven thickness distribution in the geometry is uneven compaction pressure during core expansion. A FEM approach is developed to predict the occurrence of non-conformities in the bottle. Hyperelastic core material is modelled using Mooney-Rivlin material model from the elastic strain density function. The model can be used to optimize the core shape, thus developing a robust tooling solution.

© 2019 The Authors. Published by Elsevier B.V.

This is an open access article under the CC BY-NC-ND license (<https://creativecommons.org/licenses/by-nc-nd/4.0/>)

Selection and peer-review under responsibility of the scientific committee of the 16th Global Conference on Sustainable Manufacturing (GCSM).

*Keywords:* Finite Element Modelling; Packaging; Paper moulding; Tooling

---

## 1. Introduction

Most of the packaging products today are plastic-based. Plastics impose a huge threat to the environment especially in terms of degradation [1]. However, in recent years, due to constant thrive towards sustainability, a demand in eco-friendly products has significantly increased [2]. Moulded paper pulp is mostly used in the packaging industry due to its fantastic sustainable qualities [3]. Although paper moulding can be done using many different technologies and methods, the basic principles behind are the same and can be summarized in two steps: formation of fiber network from the pulp suspension and elimination of water [4].

One example of such a product is the Green fiber Bottle (GFB). GFB is a paper bottle intended to be used for carbonated beverages [5] [6]. The work carried out in this paper introduces a FEM model to assess the quality of the compaction phase within the paper bottle production process. A critical element in manufacturing process is the

---

\*Corresponding author

*E-mail address:* [prasax@mek.dtu.dk](mailto:prasax@mek.dtu.dk)

use of inflatable core to compact the paper fibers in a bottle shape. Previous investigations on the moulding process reported non-conformities in the paper bottle due to the core insertion [7]. A FEM model has been developed and presented in this work which examines the inflatable core assisted process. The core is modelled as a hyperelastic material. Mooney-Rivlin 2 parameter hyperelastic model is used to define the material properties. The assessment of the manufacturing process gives an approach for developing a robust tooling solution.

### Nomenclature

GFB	Green fiber Bottle
W	Strain energy
$C_{10}$	Mooney-Rivlin co-efficient
$C_{01}$	Mooney-Rivlin co-efficient
I	Invariant
D	Constant, to be determined from curve-fitting
J	Jacobian
$\sigma_1$	First principal cauchy stress
$\lambda_1$	Stretch ratio
$\sigma_1^{eng}$	Engineering stress
$\epsilon_{vol}$	Volumetric strain

## 2. Manufacturing process

The conventional paper bottle moulding process is a two staged process; the forming and the drying step. In the forming process, the wet geometry is formed from paper pulp. Water is present in the pulp in two forms (a) Free water and (b) Bound water. The water that is absorbed by the pulp fibers is known as bound water, while the water that is available in excess is termed as free water. In the forming phase, free water is removed from the pulp, resulting in a wet geometry. Once the wet geometry is formed, it is then dried in sequence of steps, removing all the bound water content, as shown in fig. 1. The manufacturing process is described below:

### 2.1. Forming process

The forming process begins with injection of the pulp inside a split mould cavity (fig. 1a). The set of moulds form a negative replica of the bottle shape to be produced. The mould is setup such as the pulp enters from the neck section and the bottle is formed upside down. The pulp is kept inside a tank and continuously stirred to avoid precipitation of fibers. It is then fed into the forming mould with the help of a pump. The tool is provided with larger holes for efficient removal of the 'free water'. A wired mesh in the shape of bottle is placed at the inner lining of the mould. The dimension of mesh is such that it allows water to pass through but it doesn't allow the fibers to go out, thereby forming the shape.

With the pulp being pumped in, a pressure differential is created across the walls of the tool using vacuum suction. This process continues for a short span of time, to ease the formation of the bottle shape. Once the shape has been formed, the vacuum suction is turned off and the wet bottle is removed from the mould.

### 2.2. Drying process

This wet bottle is then transferred to a drying mould for the drying process (fig. 1b). The drying mould is also a split mould made of porous material. The porous mould is preheated to the temperature of 140 °C. As the wet paper bottle comes in contact with the hot tool, the drying process starts. During the drying process, an inflatable core/insert is inserted and inflated inside the mould. The core is made up of a rubber material. The core serves two purposes: (a) Compaction of the wet fibers and (b) Avoiding the shrinkage of paper during the drying process. A pressure differential

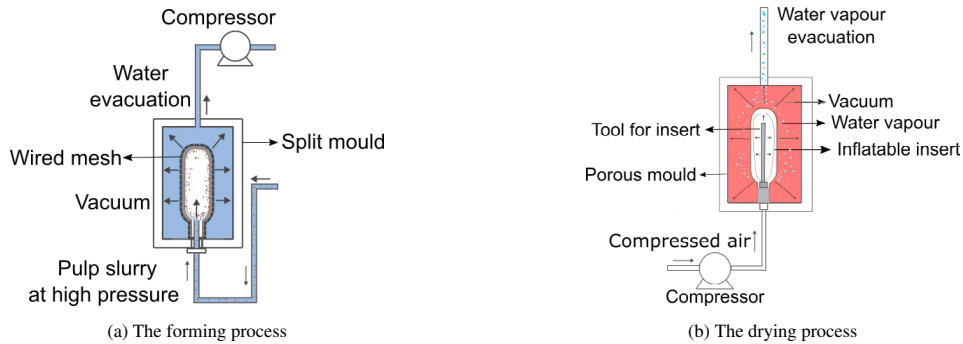


Fig. 1: Schematic showing the paper bottle manufacturing process

is created across the walls of the tool using vacuum suction. Once the drying process is completed the split mould opens up and the dried paper bottle is obtained.

### 3. Non-conformities due to inflatable core

Saxena et al.[7] performed a study on characterizing the green fiber bottle prototypes using computed tomography. The authors produced paper bottles with the manufacturing process discussed in section 2. The study revealed non-conformities in the paper bottle. The uneven thickness distribution across the length of the bottle suggested that the pulp fiber is unevenly compacted. One of the primary cause of uneven thickness distribution is the uneven compaction pressure during the drying process. Section 4 provides a method to analyze and predict the compaction pressure from the core onto the paper during manufacturing.

### 4. FEM modelling of the inflatable core assisted process

This section presents a FEM based approach for predicting non-conformities in the bottle moulding process. The inflatable core is modelled as hyperelastic material and inflated inside the mould. The FEM simulations were performed in COMSOL Multiphysics 5.3a.

#### 4.1. Model definition

The inflatable core is held between two halves of the mould as shown in fig 2. The two halves of the mould are clamped together and held stationary (Fig 2a). Pressure is applied on the inner boundary of the core and is slowly ramped up to resemble the actual manufacturing process. As the core inflates inside the mould, contact pressure between the core and the mould is evaluated. It is assumed that the pressure exerted by the core on the mould is same as that exerted by the core onto paper surface. The 3D model is reduced to 2D axi-symmetric for faster computation (fig 2b).

#### 4.2. Constitutive equations

The rubber material is modelled using Mooney-Rivlin hyperelastic model. The material is assumed to be incompressible. The model express the mechanical strain energy as a function of invariants (eq. 1).

$$W = \sum_i \sum_j C_{ij} (I_1 - 3)^i (I_2 - 3)^j + D(J - 1)^2 \quad (1)$$

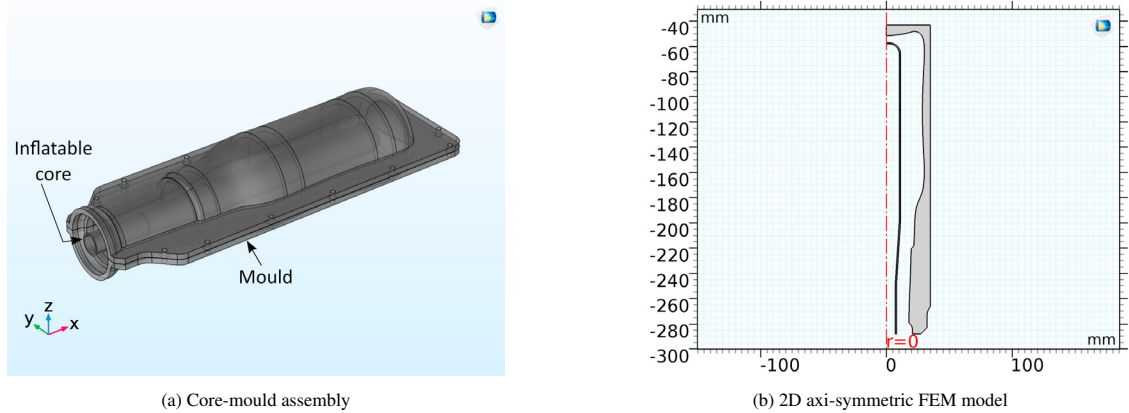


Fig. 2: FEM model setup in COMSOL

where  $C_{ij}$  and  $D$  are the constants to be determined by curve-fitting from the experimental stress-stretch curves. It is significant to note here that the above expression doesn't have a term of  $I_3$ . This is because, for incompressible materials  $I_3$  is 1. The expansion of eq. 1 gives:

$$W = C_{10}(I_1 - 3) + C_{01}(I_2 - 3) + C_{11}(I_1 - 3)(I_2 - 3) + C_{20}(I_1 - 3)^2 + \dots + D(J - 1)^2 \tag{2}$$

The partial derivative of  $W$  with respect to  $\lambda_i$ , multiplied by  $\lambda_i$  gives the principal cauchy stress. The first principal cauchy stress can be evaluated as:

$$\sigma_1 = \lambda_1 \frac{\partial W}{\partial \lambda_1} = \lambda_1 \left( \frac{\partial W}{\partial I_1} \frac{\partial I_1}{\partial \lambda_1} + \frac{\partial W}{\partial I_2} \frac{\partial I_2}{\partial \lambda_1} + \frac{\partial W}{\partial J} \frac{\partial J}{\partial \lambda_1} \right) \tag{3}$$

In common practice, Mooney Rivlin 2 parameter, 3 parameter and 5 parameter model are used for modelling rubber-like materials. The model discussed in this work makes use of Mooney-Rivlin 2 parameter hyperelastic model. From an experimental point of view, engineering stress hold much more relevance than principal cauchy stress. Engineering stress can be obtained from the first principal cauchy stress as:

$$\sigma_1^{eng} = \frac{\sigma_1}{\lambda_1} \tag{4}$$

since  $J = \frac{V_F}{V_o}$ , the expression  $(J - 1)$  in eq. 2 can be replaced with volumetric strain ( $\epsilon_{vol}$ ) as:

$$(J - 1) = \frac{\Delta V}{V_o} = \epsilon_{vol} \tag{5}$$

### 4.3. Material modelling

The mechanical behaviour of the rubber material is determined by uniaxial tensile testing. The stress-stretch behaviour for the material was determined using the testing procedure as prescribed in DIN 53504-85. Stretch is defined as:

$$Stretch = 1 + Strain. \tag{6}$$

For Uniaxial tension,

$$\lambda_1 = \lambda \tag{7}$$

$$\lambda_2 = \lambda_3 = \frac{1}{\sqrt{\lambda}} \tag{8}$$

Thus,

$$\sigma_{uniaxial}^{eng} = 2C_{10}\left(\lambda - \frac{1}{\lambda^2}\right) + 2C_{01}\left(1 - \frac{1}{\lambda^3}\right) \quad (9)$$

Fig. 3 shows the experimental stress-stretch behaviour of the rubber material in uniaxial tensile testing conditions. The experimental data is curve-fitted using Mooney-Rivlin 2 parameter model. The coefficients obtained from the curve-fitting are  $C_{01} = 0.79$  MPa and  $C_{10} = 0.52$  MPa. Other relevant material properties as obtained from the material datasheet are listed in table 1. The mould is assigned aluminium with the material properties as listed in table 2.

Table 1: Material properties of the core

Material characteristics	Value	Test standard
Hardness Shore A	30	DIN 53505
Density	1100 kg/m <sup>3</sup>	DIN EN ISO 1183-1 A
Tensile strength	8.60 N/mm <sup>2</sup>	DIN 53504 S 1
Elongation at break	650 %	DIN 53504 S 1
Tear strength	31 N/mm	ASTM D 624 B

Table 2: Material properties of the mould

Material characteristics	Value
Density	2700 kg/m <sup>3</sup>
Young's modulus	70,000 MPa
Poisson's ratio	0.33

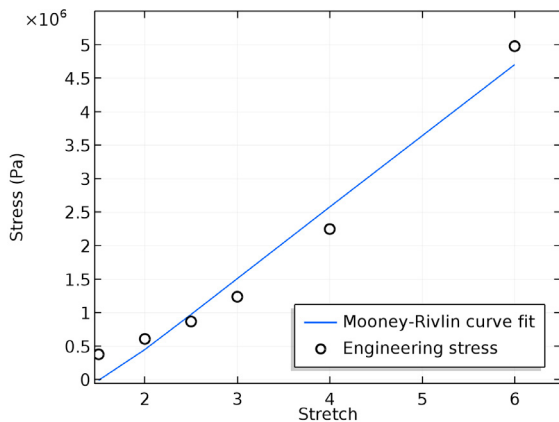


Fig. 3: Parameter estimation from curve fitting

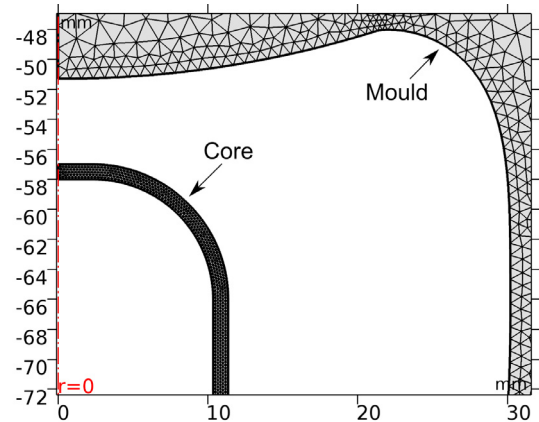


Fig. 4: Mesh elements

The design is related to a specific test geometry that was used as a basis for investigation.

#### 4.4. Meshing

The choice of right set of mesh elements is very critical in modelling hyper-elastic materials. Triangular mesh elements are used for both the core and the mould (fig. 4). The maximum size of mesh elements for the core is 0.22 mm. The inner part of the mould that comes in contact with the core is meshed with the elements of size 0.8 mm.

#### 4.5. Boundary constraints and load

In order to allow expansion of the core, the lower part of the core is provided with a roller boundary condition. The mould is provided with the fixed domain constraint. The outer boundary of core and the inner boundary of tool forms a contact pair. The inner boundary of the core is provided a boundary load (pressure) which is slowly ramped up to avoid large distortion of mesh elements in one step.

The rubber core expansion inside the mould is a boundary value problem. The deformation of the core is defined from the moving mesh boundaries. The strain in rubber material is defined at each point in the domain. A positive volumetric change means the core is stretched, while a negative value indicates compression. The total mass however remains conserved at all times.

### 5. Results

As the applied pressure is ramped up, the core begins to inflate and after sometime contact is established with the mould surface. The contact pressure is evaluated as a measure of uniformity of pressing and fibers compaction. Fig 5a shows the distribution of contact pressure with the applied pressure. As it can be seen, when nearly 7 bar ( $7 \times 10^5$  Pa) of pressure is applied inside the core, the contact pressure on the largest fraction of the mould surface is approximately 4.5 bar ( $4.5 \times 10^5$  Pa) (shown with dark blue colour).

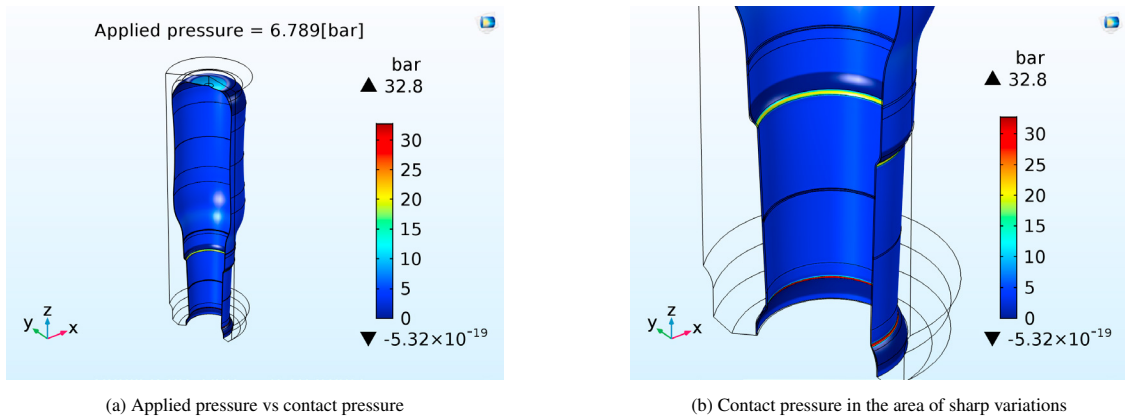


Fig. 5: Contact pressure in the tool

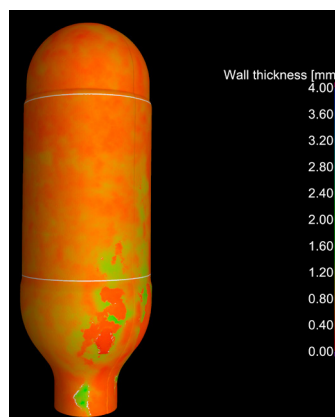


Fig. 6: Wall thickness analysis of a paper bottle [7]

However, it can be seen from fig. 5b that in the area of sharp variations of cross section, characterized by a small curvature radius, the contact pressure is non-uniform. The sharp curvatures in the mould makes it difficult for the core to maintain uniform contact pressure in the tool. This generates the zone of non-conformities, verified by Saxena et al. [7].

In concave corners, where the contact pressure is relatively low, the rubber core is unable to compact the pulp uniformly, thereby leaving more thickness in that region. However, in convex corners, where the contact pressure is relatively high, the pulp is compacted more, generating the regions of low thickness. The thickness distribution from the study by Saxena et al. [7] is shown in fig 6.

## 6. Conclusions

The paper presents an approach to estimate and predict the non-conformities during the paper bottle moulding process. Following points can be concluded from the work:

- The expansion of core inside the mould cavity generates contact pressure on the paper surface.
- This contact pressure helps in removal of bound water, absorbed by the paper fibers and also allows good compaction.
- There is significant deviation in the contact pressure from the applied pressure.
- The FEM model provides the distribution of contact pressure during compaction. The distribution of contact pressure is observed to be non-uniform.
- The core produces a good compaction in most of the bottle, however, it is unable to provide uniform compaction in the area of sharp variations of cross section.
- The model can be used as a selection criteria in choosing the core material.
- The shape of core can be modified and validated from the model, such as the contact pressure is uniformly distributed across the bottle.
- The cause of non-conformities in the bottle production is confirmed as pointed out in earlier studies.

Thus, with the help of the FEM model, the manufacturing process can be tuned accordingly. The tools can be more accurately designed to have a robust and sustainable manufacturing process for production cycle.

## 7. Acknowledgements

The work carried out in this paper is funded by Innovations Fund Denmark, grant no. 5106-00006B furnished for the project titled "Impulse Drying of cardboard moulded 3D structures". The authors would like to thank Morten Siwertsen from COMSOL A/S, Denmark for all his help and support in performing the FEM simulations. The motivation and support from EcoXpac and Carlsberg group is also acknowledged.

## References

- [1] H. Webb, J. Arnott, R. Crawford, E. Ivanova, Plastic Degradation and Its Environmental Implications with Special Reference to Poly(ethylene terephthalate), *Polymers*, 5(1) (2013) 1-18.
- [2] R. Wever, D. Twede, The history of molded fiber packaging; a 20th century pulp story, *Proceedings of the 23rd IAPRI symposium on packaging*, (2007).
- [3] M. Didone, P. Saxena, E.B. Meijer, G. Tosello, G. Bissacco, T.C. McAloone, D.C.A. Pigosso, T.J. Howard, Moulded Pulp Manufacturing: Overview and Prospects for the Process Technology, *Packaging Technology and Science*, 30(6) (2017) 231-249.
- [4] R.W. Emery, J.R. Emery, Review of the pulp molding industry and processes used, *Paper Trade*, (1966) 29-33.
- [5] M. Didone, G. Tosello, T.J. Howard, Green fiber bottle: Towards a sustainable package, *16th Fundamental Research Symposium: Advances in Pulp and Paper Research*, Oxford, United Kingdom, (2017).
- [6] P. Saxena, G. Bissacco, F.J. Bedka, A. Stolfi, Tooling for Production of the Green Fiber Bottle, *Procedia CIRP*, 69 (2018) 348-353.
- [7] P. Saxena, G. Bissacco, A. Stolfi, L.De. Chiffre, Characterizing Green Fiber Bottle Prototypes Using Computed Tomography, *Proceedings of the 7th Conference on Industrial Computed Tomography*, (2017).